



## **Biomimetic Approach to Solar Cells Based on TiO<sub>2</sub> Nanotubes**

**by Jan L. Allen, Ivan C. Lee, and Jeff Wolfenstine**

**ARL-TN-312**

**April 2008**



## **NOTICES**

### **Disclaimers**

The findings in this report are not to be construed as an official Department of the Army position unless so designated by other authorized documents.

Citation of manufacturer's or trade names does not constitute an official endorsement or approval of the use thereof.

Destroy this report when it is no longer needed. Do not return it to the originator.



# **Army Research Laboratory**

Adelphi, MD 20783-1197

---

---

**ARL-TN-312**

**April 2008**

---

## **Biomimetic Approach to Solar Cells Based on TiO<sub>2</sub> Nanotubes**

**Jan L. Allen, Ivan C. Lee, and Jeff Wolfenstine  
Sensors and Electron Devices Directorate, ARL**



REPORT DOCUMENTATION PAGE				Form Approved OMB No. 0704-0188	
Public reporting burden for this collection of information is estimated to average 1 hour per response, including the time for reviewing instructions, searching existing data sources, gathering and maintaining the data needed, and completing and reviewing the collection information. Send comments regarding this burden estimate or any other aspect of this collection of information, including suggestions for reducing the burden, to Department of Defense, Washington Headquarters Services, Directorate for Information Operations and Reports (0704-0188), 1215 Jefferson Davis Highway, Suite 1204, Arlington, VA 22202-4302. Respondents should be aware that notwithstanding any other provision of law, no person shall be subject to any penalty for failing to comply with a collection of information if it does not display a currently valid OMB control number. <b>PLEASE DO NOT RETURN YOUR FORM TO THE ABOVE ADDRESS.</b>					
1. REPORT DATE (DD-MM-YYYY) April 2008		2. REPORT TYPE Final		3. DATES COVERED (From - To) October 2006–September 2007	
4. TITLE AND SUBTITLE Biomimetic Approach to Solar Cells Based on TiO <sub>2</sub> Nanotubes				5a. CONTRACT NUMBER	
				5b. GRANT NUMBER	
				5c. PROGRAM ELEMENT NUMBER	
6. AUTHOR(S) Jan L. Allen, Ivan C. Lee, and Jeff Wolfenstine				5d. PROJECT NUMBER FY07-SED-01	
				5e. TASK NUMBER	
				5f. WORK UNIT NUMBER	
7. PERFORMING ORGANIZATION NAME(S) AND ADDRESS(ES) U.S. Army Research Laboratory ATTN: AMSRD-ARL-SE-DC Adelphi, MD 20783-1197				8. PERFORMING ORGANIZATION REPORT NUMBER ARL-TN-312	
9. SPONSORING/MONITORING AGENCY NAME(S) AND ADDRESS(ES)				10. SPONSOR/MONITOR'S ACRONYM(S)	
				11. SPONSOR/MONITOR'S REPORT NUMBER(S)	
12. DISTRIBUTION/AVAILABILITY STATEMENT Approved for public release; distribution is unlimited.					
13. SUPPLEMENTARY NOTES					
14. ABSTRACT The goal of this research was to explore the use of nanotube titanium dioxide (TiO <sub>2</sub> ) as an electrode material in dye-sensitized solar cells in order to further the development of solar cell technology. TiO <sub>2</sub> nanotubes were successfully synthesized by hydrothermal methods, working solar cells were constructed, and comparisons were made between nanospherical TiO <sub>2</sub> and nanotubular TiO <sub>2</sub> . The results showed an increase in the maximum photocurrent density, J <sub>sc</sub> , at the expense of a lowered fill factor that led to a lowered cell efficiency. It is suggested that improvements can be realized by the use of aligned TiO <sub>2</sub> nanotubes in order to enable a higher packing density of the nanotubes that would lead to a higher photocurrent density per square centimeter, thereby converting a portion of the incoming solar energy into electrical energy.					
15. SUBJECT TERMS solar cell, dye sensitized, TiO <sub>2</sub> , nanotubes, titanium dioxide, photovoltaic, power generation, titanium (IV) oxide, biomimetic					
16. SECURITY CLASSIFICATION OF:			17. LIMITATION OF ABSTRACT  UL	18. NUMBER OF PAGES  16	19a. NAME OF RESPONSIBLE PERSON Jan L. Allen
a. REPORT UNCLASSIFIED	b. ABSTRACT UNCLASSIFIED	c. THIS PAGE UNCLASSIFIED			19b. TELEPHONE NUMBER (Include area code) 301-394-0291



---

## Contents

---

<b>List of Figures</b>	<b>iv</b>
<b>List of Tables</b>	<b>iv</b>
<b>1. Objective</b>	<b>1</b>
<b>2. Approach</b>	<b>1</b>
<b>3. Results</b>	<b>2</b>
3.1 TiO <sub>2</sub> Nanotube Synthesis .....	2
3.2 TiO <sub>2</sub> Nanotube Characterization .....	2
3.3 Electrode Preparation .....	3
3.4 Cell Assembly .....	5
3.5 Solar Cell Characterization .....	5
<b>4. Conclusions</b>	<b>8</b>
<b>Distribution List</b>	<b>9</b>



---

## List of Figures

---

Figure 1. X-ray diffraction pattern of hydrothermal product. The x-ray shows the anatase form of $\text{TiO}_2$ . The broad peaks are indicative of a nanosized material. The analysis of line broadening by the Sherrer equation gave a crystallize size of about 10 nm. ....	3
Figure 2. SEM image of $\text{TiO}_2$ nanotubes prepared by the hydrothermal method. The tube diameter is $<100$ nm, and the lengths are $>3$ $\mu\text{m}$ . ....	3
Figure 3. An example of a coating of $\text{TiO}_2$ on conductive (F-doped $\text{SnO}_2$ -coated) glass. ....	4
Figure 4. $\text{TiO}_2$ film adsorbing the solar dye. ....	5
Figure 5. Assembled solar cell connected for measurement of photocurrent-voltage (I-V) curve. ....	6
Figure 6. The new ARL solar cell I-V curve testing system. ....	6
Figure 7. Typical I-V curve. ....	7

---

## List of Tables

---

Table 1. I-V characteristics (under sun AM 1.5 illumination for cells with various morphologies and mixtures of $\text{TiO}_2$ ). ....	7
--	---



---

## 1. Objective

---

The goal of the research was to explore the use of nanotube  $\text{TiO}_2$  as an electrode material in dye-sensitized solar cells in order to further the development of solar cell technology.

---

## 2. Approach

---

All photoelectric devices capture solar energy by the generation of a higher-energy mobile electron upon illumination by the sun. The mobile electron can be harnessed to create electricity; however, in a semiconductor-based solar cell, the mobile electron leaves behind a positive hole within the material that can recombine with the electron, thus reducing efficiency. For the case of a semiconductor photocell, an electric field is used to reduce this recombination.<sup>1</sup> These carriers are then transported to electrodes where they become the basis of an electrical current. Current state-of-the-art high-efficiency cells use a combination of semiconductors with different band gaps to capture a larger portion of the solar spectrum. Although the efficiency of some of these advanced photovoltaic cells is high with conversion efficiencies nearing 50%, the main drawback of these technologies is the high cost. In addition, semiconductor-based solar cells do not work well under low-light conditions where they suffer a “cutout” at some lower limit of illumination, when charge carrier mobility is low and recombination becomes a major issue. However, there is another method to separate the electron and holes that mimic the method of photosynthesis. These cells are called dye-sensitized solar cells or DSSCs.<sup>2</sup> As a result of low losses and a lack of recombination unlike semiconductor-based systems, DSSCs work even in low-light, cloudy sky conditions. In addition, they are fabricated using inexpensive processing methods and materials. Furthermore, the cells can be made flexible. These features will be critical to the warfighter needing to fight under all weather conditions.

In general, a DSSC is a composite material in which a mobile electron is created via a dye, and the electron is transported away via semiconducting  $\text{TiO}_2$ . Typically, nanoparticle  $\text{TiO}_2$  is used as the electrode because of its high surface area.<sup>2</sup> However, one of the major limitations of dye-sensitized solar cells is reduced efficiency as a result of poor electron transport. The structural disorder at contact between nanoparticles leads to enhanced scattering of free electrons, thus reducing electron mobility, hence reducing efficiency. It is goal of the proposed work to show that by changing the architecture of the  $\text{TiO}_2$  from a nanoparticle to a nanotube, the electrode

---

<sup>1</sup> Chapin, D. M.; Fuller, C. S.; Pearson, G. L. A New Silicon P-N Junction Photocell for Converting Solar Radiation Into Electrical Power. *J. Appl. Phys.* **1954**, 25, 676.

<sup>2</sup> O'Regan, B.; Grätzel, M. A Low-Cost, High Efficiency Solar Cell Based on Dye-Sensitized Colloidal  $\text{TiO}_2$  Films. *Nature* **1991**, 353, 737–740.



material will retain the needed high surface area but reduce the number of interparticle contacts, hence increasing electron mobility and cell efficiency.

---

### 3. Results

---

#### 3.1 TiO<sub>2</sub> Nanotube Synthesis

TiO<sub>2</sub> nanotube synthesis was attempted by hydrothermal methods and by anodic oxidation of titanium foil and titanium sputter coated onto conductive glass. Initial experimentation and characterization suggested that the hydrothermal method would be most expedient within the time constraints. Further work will be required to optimize the anodic oxidation process as there is a competition between formation of TiO<sub>2</sub> and the dissolution of the TiO<sub>2</sub> into the etching solution, which is generally HF based. The sputter-coated samples did not adhere well enough to the substrate and tended to peel off during the oxidation step. The successful hydrothermal method of synthesis is detailed below.

Step 1.  $\text{TiO}_2 + 2\text{NaOH} \rightarrow \text{Na}_2\text{TiO}_3 \text{ (nanotubes)} + \text{H}_2\text{O}$ : The nanotubes were prepared by mixing nanophase TiO<sub>2</sub> with 10–15 M NaOH solution in a Teflon-lined autoclave. The samples were heated in the oven at different temperatures, 100, 130, 160, and 180 °C for 1–72 hr. The newly formed white suspension was separated from the liquid by centrifuge. The samples were washed at least three times with deionized water and, subsequently, the liquid phase was removed by use of the centrifuge.

Step 2. Acidification:  $\text{Na}_2\text{TiO}_3 + \text{H}^+ \rightarrow \text{H}_2\text{TiO}_3 \text{ (nanotube)}$ : The sample was stirred with an aqueous 0.1 M HCL solution for about 1–2 hr in order to exchange Na<sup>+</sup> with H<sup>+</sup>. Afterward, the sample was washed at least three times with distilled water via centrifugation. The washed H<sub>2</sub>TiO<sub>3</sub> nanotubes were then dried overnight at 40–80 °C, which removed the excess water.

Step 3. Thermal dehydration:  $\text{H}_2\text{TiO}_3 \rightarrow \text{TiO}_2 \text{ (nanotube)} + \text{H}_2\text{O}$ : The dried H<sub>2</sub>TiO<sub>3</sub> was then thermally dehydrated at 400 °C to form nanotubular TiO<sub>2</sub>. In a few cases, the sample was left in the protonic form, and the dehydration step was done concurrently with the sintering step of the solar cell electrode fabrication.

#### 3.2 TiO<sub>2</sub> Nanotube Characterization

X-ray diffraction was done using a Rigaku Ultima 3 diffractometer with Cu-Kα radiation (operated at 44 kV, 40 mA) to identify the TiO<sub>2</sub> phase and to provide an estimate of crystallite size through use of the Sherrer equation. The x-ray diffraction pattern in figure 1 shows only peaks corresponding to the anatase form of TiO<sub>2</sub>. The broad peaks are indicative of a nanosized material. The analysis of line broadening by the Sherrer equation gave a crystallite size of about



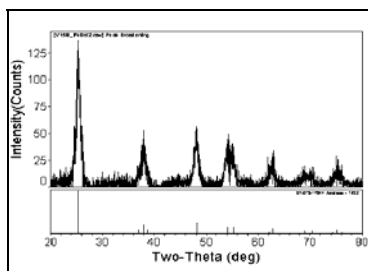


Figure 1. X-ray diffraction pattern of hydrothermal product. The x-ray shows the anatase form of  $\text{TiO}_2$ . The broad peaks are indicative of a nanosized material. The analysis of line broadening by the Sherrer equation gave a crystallize size of about 10 nm.

10 nm. Surface area was measured by the BET method. Surface areas of  $48.4 \pm 0.2$  and  $54.5 \pm 0.2 \text{ m}^2/\text{g}$  were measured for the U.S. Army Research Laboratory (ARL) nanotubes and a  $\text{TiO}_2$  control of spherical morphology (P25, Degussa), respectively.

Scanning electron microscopy (SEM) was used to evaluate the morphology of the  $\text{TiO}_2$ . Figure 2 shows a representative image of nanotubes formed by the hydrothermal method. The bar at the bottom of the image is  $4 \mu\text{m}$ . The diameter is shown to be  $<100 \text{ nm}$ , and the lengths are  $>3 \mu\text{m}$ . There is also evidence of the agglomerations of individual tubes into larger bundles.

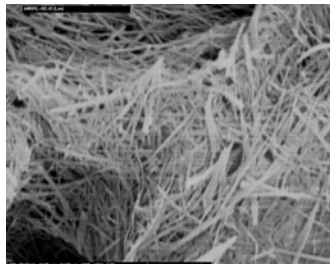


Figure 2. SEM image of  $\text{TiO}_2$  nanotubes prepared by the hydrothermal method. The tube diameter is  $<100 \text{ nm}$ , and the lengths are  $>3 \mu\text{m}$ .

### 3.3 Electrode Preparation

The first step to electrode preparation was to coat a layer of the  $\text{TiO}_2$  onto a conductive glass substrate (F-doped  $\text{SnO}_2$ -coated glass, Hartford Glass). The coatings were optimized by varying the ratio of  $\text{TiO}_2$ , solvent, and binder. Two systems were explored: an aqueous system using water-soluble hydroxyethylcellulose as binder and an organic solvent system using terpeneol as solvent and ethyl cellulose as binder. The aqueous system was optimized with a mass percent of 15.9%, 4.8%, and 79.3% of  $\text{TiO}_2$ , hydroxyethylcellulose, and water, respectively. The terpeneol-based system was optimized with a mass percent of 17.7%, 4.3%, and 79.4% of  $\text{TiO}_2$ , ethylcellulose, and terpeneol, respectively. Preliminary solar cell testing indicated slightly better



performance for the aqueous system, thus it was chosen for further coatings. Better dispersion during the mixing phase was noted when using a slightly acidic aqueous solution (0.1 M acetic acid) to mix with the  $\text{TiO}_2$  and cellulosic binder. After the formulations were optimized on glass microscope slides, coatings were then done on the conductive glass slides. For optimal solar cell efficiency, the conductive glass slides were pretreated with  $\sim 1 \text{ drop/cm}^2$  of 50 mM  $\text{TiCl}_4$  (aq). Care was taken to only treat the area of the conductive glass to be coated, and the solution was dried prior to coating with the  $\text{TiO}_2$  paste. The area to be coated was bounded by Scotch tape, which provides about the right thickness of electrode if two coating and drying cycles are done. Alternatively, two layers of Scotch tape can be used with one coating. The coating thickness was around  $10 \text{ }\mu\text{m}$ , as measured by a profilometer. An example of a coated electrode is shown in figure 3.



Figure 3. An example of a coating of  $\text{TiO}_2$  on conductive (F-doped  $\text{SnO}_2$ -coated) glass.

Several methods of drying the  $\text{TiO}_2$  paste were considered, including drying at ambient, drying in an  $80^\circ\text{C}$  oven with circulating air, and drying under an infrared lamp with static air. The infrared lamp was chosen to be the most time efficient and also dried the sample at a rate that was not too fast, which would lead to peeling of the coating.

The next step involved sintering the coating. During this step, the cellulosic binder is removed by carbonization and subsequent oxidation to  $\text{CO}_2$ . The  $\text{TiO}_2$  nanoparticles/tubes are then sintered at  $450\text{--}500^\circ\text{C}$  to form connections to allow a more efficient electron-conductive network while maintaining a porosity and surface area sufficient to adsorb the dye. The sintered electrode is then treated with  $\sim 1 \text{ drop/cm}^2$  of 50 mM  $\text{TiCl}_4$  (aq). This coating helps to provide a surface rich in titanium rather than oxygen, which allows a ready bonding of the dye to the surface of the photoelectrode. The electrode is held at  $80^\circ\text{C}$  for at least 30 min after the  $\text{TiCl}_4$  treatment.

After the  $\text{TiO}_2$  has been sintered, it is now time to apply the dye to the films. The  $\text{TiO}_2$  nanotubes were coated with a 0.3 mM dry acetonitrile solution of Solaronix N719 dye [Cis-di (thiocyanato) bis (2, 2'-bipyridyl-4, 4'-dicarboxylate) ruthenium (II)] to form a composite material. The dye was chosen because it has high-energy conversion efficiency and



high photo- and chemical stability.<sup>3</sup> The dye solution was placed in a petri dish, then the TiO<sub>2</sub> film was placed into the dish to absorb the dye as shown in figure 4. The coating was submerged in the dye for a minimum of 24 hr. Better results are obtained by submerging the coated conductive glass substrate directly from the 80 °C oven. This prevents undue absorption of ambient moisture and thereby increases the available sites for dye absorption. The dye impregnation steps were done in a dry room with a dewpoint of < -80 °C to further ensure that moisture did not absorb onto the TiO<sub>2</sub> in place of the dye. After impregnation, the sample is removed, rinsed with acetonitrile, and dried prior to cell assembly.



Figure 4. TiO<sub>2</sub> film adsorbing the solar dye.

### 3.4 Cell Assembly

First, the counterelectrode was sputter coated with platinum on the conductive side of a glass slide. The platinum serves as a catalyst that regenerates the triiodide-based electrolyte during cell operation. Second, sandwich cells were constructed by using the dye-anchored TiO<sub>2</sub> film as a working electrode and a platinum-coated conducting glass as a counterelectrode. The electrodes were superimposed with a thin Teflon gasket between the electrodes to prevent shorting. Iodide/triiodide redox electrolyte (Iodolyte TG50, Solaronix) was introduced into the space between the electrodes. The two electrodes were offset to allow ohmic contact and were held together by small binder clips. An assembled cell is shown in figure 5.

### 3.5 Solar Cell Characterization

New test equipment for measuring the solar cell photocurrent-voltage (I-V) curve was purchased and installed as part of the Director's Research Initiative (DRI). Before the DRI, there was not an existing capability at ARL. The ARL solar cell I-V curve testing system defines the I-V characteristics of photovoltaic devices with dimensions up to 5 × 5 cm and currents up to 3 A. The system includes a solar simulator designed to have a constant solar irradiance of 100 mW/cm<sup>2</sup>, allowing a standardized test condition. The system enables the calculation of solar

---

<sup>3</sup>Nazeeruddin, Md. K.; Humphry-Baker, R.; Grätzel, M. Investigation of Sensitizer Adsorption and the Influence of Protons on Current and Voltage of a Dye-Sensitized Nanocrystalline TiO<sub>2</sub> Solar Cell. *J. Phys. Chem. B* **2003**, *107*, 8981.





Figure 5. Assembled solar cell connected for measurement of photocurrent-voltage (I-V) curve.

cell parameters including open circuit voltage ( $V_{oc}$ ), short circuit current ( $I_{sc}$ ), current per  $cm^2$  ( $J_{sc}$ ), voltage maximum ( $V_{max}$ ), current maximum ( $I_{max}$ ), power maximum ( $P_{max}$ ), fill factor (FF), and efficiency, and will be useful for all further photovoltaic work at ARL. The measurement system is shown in figure 6.



Figure 6. The new ARL solar cell I-V curve testing system.

For comparison, a standard  $TiO_2$  of spherical morphology (P25, Degussa) was used to build control samples. The test cells included nanotubular  $TiO_2$  prepared by hydrothermal methods at ARL, mixtures of nanotubular  $TiO_2$  and P25, and a bilayer structure of a first coating of P25 and a second coating of nanotubular  $TiO_2$ . The results are shown in table 1. A typical I-V curve is shown in figure 7 with current on the vertical axis and voltage on the horizontal axis.



Table 1. I-V characteristics (under sun AM 1.5 illumination for cells with various morphologies and mixtures of TiO<sub>2</sub>).

Cell Characteristics	BET Surface Area (m <sup>2</sup> /g)	J <sub>sc</sub> (mA/cm <sup>2</sup> )	V <sub>oc</sub> (V)	FF (%)	Efficiency (%)
P25 TiO <sub>2</sub> (control)	54.5	4.26	0.756	61.6	1.98
ARL nanotubes	48.4	1.52	0.745	64.7	0.73
P25: nanotube; 1:1	—	5.14	0.680	37.6	1.31
P25: nanotube bilayer	—	4.87	0.713	43.7	1.52

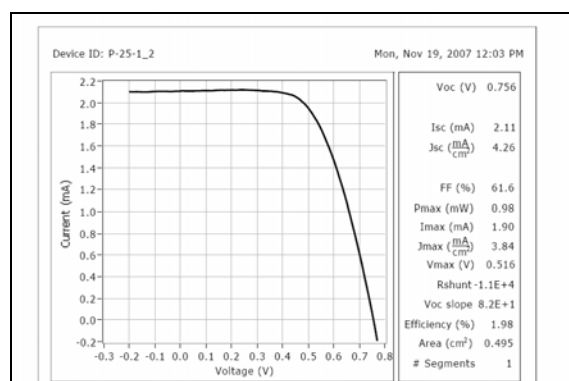


Figure 7. Typical I-V curve.

From table 1, note that the highest efficiency was measured for the P25 nanospherical TiO<sub>2</sub>. The current density was much lower for the ARL nanotubes. It is believed that the reduced current density results from a reduced packing density of the tubes relative to the spheres. Their less compact packing results in a significant decrease in available surface area for dye adsorption, thus decreasing the current density. In order to use nanotubular TiO<sub>2</sub> as an electrode material by itself, it may be necessary to either synthesize tubes with higher surface area or synthesize aligned tubes because aligned tubes can have a higher packing density than spheres. The highest possible packing density of spheres is 0.74 (on a scale of 0 to 1), whereas for aligned tubes, a packing density of 0.9 is possible. Anodic oxidation is a possible fabrication method for aligned tubes. In addition, the electrode processing can be modified to produce thicker films to compensate for the loss of surface area. Mixtures of P25 TiO<sub>2</sub> and the ARL nanotubular TiO<sub>2</sub> showed the highest current density, J<sub>sc</sub>, thus suggesting that the electron mobility might be increased as was hypothesized at the beginning of this research.

Unfortunately, the mixtures including both a physical mixture of the two powders and a bilayer structure showed a considerably reduced FF, leading to a reduced photovoltaic efficiency. A reduced FF generally is a result of increases in parasitic resistances. It is believed that the reduced FF results from poor contact between the two morphologies of TiO<sub>2</sub> in the mixed



morphology electrodes. In the future, different ratios (reduced amount of nanotubes) could be tried in order to balance the tradeoffs between nanotubular  $\text{TiO}_2$  and traditional nanospherical  $\text{TiO}_2$ . Nanoparticle/nanotube composites may possess the advantages of both building blocks (the high surface area of nanoparticle aggregates and the rapid electron transport rate and light-scattering effect of single-crystalline nanotubes), but steps will need to be taken to overcome poor contact between unlike morphologies to reduce parasitic resistances.

---

## **4. Conclusions**

---

The objectives of the proposed research were met.  $\text{TiO}_2$  nanotubes were successfully synthesized by hydrothermal methods, working solar cells were constructed, and comparisons were made between nanospherical  $\text{TiO}_2$  and nanotubular  $\text{TiO}_2$ . The results showed some improvements in  $J_{sc}$  at the expense of a lowered FF and a reduced cell efficiency. Perhaps for the first time, most importantly, ARL has a photocurrent-voltage measurement system to enable rapid testing of future high-potential solar cell materials and devices for warfighter applications.



NO. OF  
COPIES ORGANIZATION

1 DEFENSE TECHNICAL  
(PDF INFORMATION CTR  
ONLY) DTIC OCA  
8725 JOHN J KINGMAN RD  
STE 0944  
FORT BELVOIR VA 22060-6218

1 DIRECTOR  
US ARMY RESEARCH LAB  
IMNE ALC IMS  
2800 POWDER MILL RD  
ADELPHI MD 20783-1197

1 DIRECTOR  
US ARMY RESEARCH LAB  
AMSRD ARL CI OK TL  
2800 POWDER MILL RD  
ADELPHI MD 20783-1197

1 DIRECTOR  
US ARMY RESEARCH LAB  
AMSRD ARL CI OK T  
2800 POWD ER MILL RD  
ADELPHI MD 20783-1197

1 DIRECTOR  
US ARMY RESEARCH LAB  
AMSRD ARL RO EV  
W D BACH  
PO BOX 12211  
RESEARCH TRIANGLE PARK  
NC 27709

ABERDEEN PROVING GROUND

1 DIR USARL  
AMSRD ARL CI OK TP (BLDG 4600)



INTENTIONALLY LEFT BLANK.